Strain-induced nonequilibrium magnetoelastic domain structure and spin reorientation of NiO(100)

Suman Mandal and Krishnakumar S. R. Menon*
Surface Physics Division, Saha Institute of Nuclear Physics, 1/AF Bidhannagar, Kolkata 700064, India

Francesco Maccherozzi and Rachid Belkhou
Synchrotron SOLEIL, L'Orme des Merisiers Saint-Aubin, 91192 Gif-sur-Yvette, France
and Sincrotrone ELETTRA, 4-km 163,5 in AREA Science Park, 34012 Basovizza, Trieste, Italy
(Received 14 July 2009; revised manuscript received 24 August 2009; published 9 November 2009)

We report the observation of strain-induced antiferromagnetic domain structure on cleaved surface of NiO single crystal. This nonequilibrium domain structure undergoes various spin reorientations (from in plane to different in plane, out of plane to in plane) after mild annealing, indicating a direct correlation between the surface strain field and domain morphology. These reorientations are found to be driven by structural modification on the surface generated by cleaving process and buried dislocations, altering the surface magnetic anisotropy and their relaxation through mild annealing. These observations establish that the magnetoelastic effect plays a dominant role in determining antiferromagnetic domain structure.

DOI: 10.1103/PhysRevB.80.184408 PACS number(s): 75.50.Ee, 75.60.Ch, 68.37.Xy, 68.47.Gh

I. INTRODUCTION

Magnetic domains occur naturally in all magnetic materials and play a vital role in determining their magnetic properties.[1] Applications in the area of magnetic data storage, magnetoelectronics and spintronic devices have enhanced the significance of surface magnetism and a detailed understanding of the magnetic microdomain structures is essential for their practical applications.[2,3] In general, there is a lack of understanding of the surface antiferromagnetic (AF) domains in comparison to their ferromagnetic counterparts, contributed largely by the limited experimental probes sensitive to surface antiferromagnetic order. The antiferromagnetic domains have different origin compared to those in ferromagnets due to their magnetically compensated nature of the spin structure and higher-order contributions such as magnetoelastic anisotropy have to be considered. Thus, antiferromagnetic domains are more susceptible to external or internal stress field[4] for their stabilization which needs to be addressed to understand their properties. There are other important effects such as the presence of perpendicular magnetocrystalline anisotropy (PMA) where surface magnetic domains have an out-of-plane orientation and spin reorientation or domain switching. The Presence of PMA and its dependence on physical variables (such as temperature and strain) governs spin reorientation transition (SRT), where the magnetic moment orientation changes from out of plane to in plane or vice versa. Realization of surface SRT on antiferromagnetic materials is significant also from technological perspective as a potential candidate for magnetic domain control in magnetoelectronic devices,[2] especially in spin-valve devices as a way to control the adjacent ferromagnetic domains using the interfacial exchange interactions or magnetic interlayer coupling.[5,6] So far, mostly ferromagnetic systems are known to exhibit these properties which are rather well characterized.[7] There have been few studies available in literature on the NiO(100) thin-film system demonstrating the presence of PMA (Ref. 8) and in-plane SRT (Ref. 9) using spectroscopic technique. However in these studies, we get only average information about the system without any local information.

Nickel Oxide (NiO) is considered to be a prototype antiferromagnetic system with bulk domain structure studied extensively, both theoretically[10,11] and experimentally.[12–14] The easy axes of the Ni moments are determined to be along $\langle 11\bar{2}\rangle$ directions and lying in the easy [111] plane leading to a ferromagnetic spin arrangement within the [111] plane with antiferromagnetic arrangement between adjacent [111] planes. The exchange striction resulting from this antiferromagnetic spin arrangement leads to a rhombohedral contraction along $\langle 111\rangle$, yielding four different twin (T) domains characterized by different rhombohedral axis. Each T domain can further split into three spin (S) domains due to the different possible $\langle 11\bar{2}\rangle$ directions. NiO crystals show large magnetoelastic effect and this magnetoelastic term primarily governs the nature of antiferromagnetic domains and the domain walls.[15] Gomonay *et al.*[4] theoretically investigated the general issues of antiferromagnetic domains and proposed that, the incompatibility between the surface and bulk magnetostriction results in "elastic charges" at the surface producing an elastic stray field, determining the equilibrium magnetic domain structure. Apart from this intrinsic surface effect, there are other nonequilibrium effects on surfaces such as strain, dislocations etc. which are expected to modify the surface antiferromagnetic domain structure via the magnetoelastic effect and can exhibit interesting phenomenon such as the presence of PMA and SRT. The motivation of the present work is to address these issues experimentally by studying the magnetoelastic nature of the antiferromagnetic domains on the freshly cleaved surface of NiO(100) expecting the presence of induced surface strain field. In the present work, we use a combination of low energy electron microscopy (LEEM) and photoemission electron microscopy (PEEM), with LEEM providing the structural and morphological information along with magnetic information obtained from x-ray magnetic linear dichroism (XMLD) as a

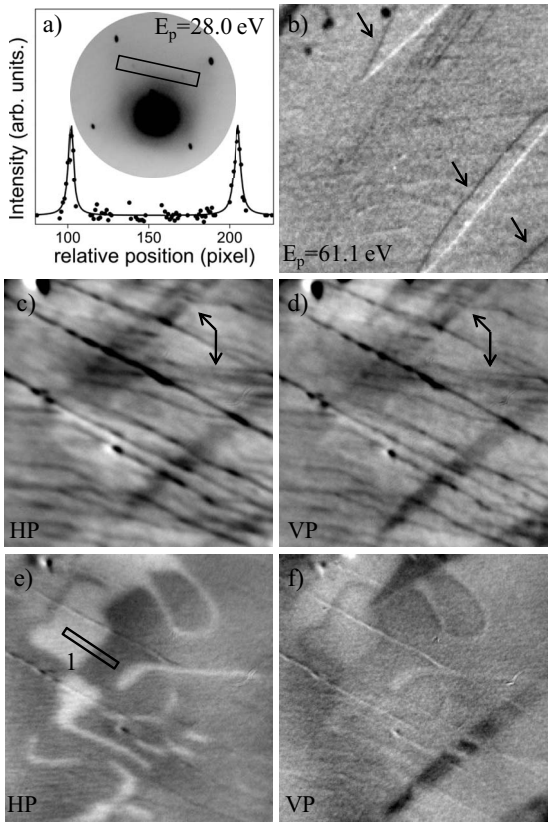

FIG. 1. (a) LEED image (28 eV) from the cleaved NiO(100) surface. Line profile along the half-order spots (marked) is shown in the main panel. (b) LEEM image obtained at 61.1 eV with a field of view=(7×7) μm^2 in overfocused condition. (c) Topography image generated from the PEEM images at the same region with HP light, (d) with VP light, (e) XMLD-PEEM image of the as-cleaved surface using HP light, and (f) using VP light.

contrast mechanism.[16] By using XMLD-PEEM, we are able to image the domain structure locally,[15,17–22] thereby giving a local information rather than an average.

II. EXPERIMENTAL DETAILS

The experiments were performed at the French branch of the Nanospectroscopy beamline at the ELETTRA storage ring using a commercial LEEM/PEEM microscope (Elmitec GmbH). The spatial resolution of the microscope in this photoemission mode (PEEM) is limited by the chromatic and spherical aberration to 25 nm, with a probing depth around 5–10 nm, depending on material used. The lateral resolution of the LEEM is better than 10 nm, and reveals the geometrical and structural features of the studied objects. NiO crystal cubes were cleaved *ex situ* and introduced into the UHV chamber soon after for the measurements without any outgassing procedures, in the "as-cleaved" condition. The cleaved surfaces were characterized by low-energy electron diffraction (LEED) measurements and the sharp (1×1) pattern in Fig. 1(a) indicate the high structural quality of the surface. Interestingly, for primary electron energies (Ep) below 35 eV, we could detect the half-order spots [see Fig. 1(a)], arising due to the exchange scattering from the antiferromagnetic lattice, as reported first by Palmberg *et al.*[23] These weak spots, with ~2% intensity of the integral spots, confirms the long-range antiferromagnetic order on the cleaved surface. The surface morphology as shown in Fig. 1(b) was acquired with Ep=61.1 eV in overfocused condition of LEEM mode. The field of view is (7×7) μm^2, which is same for all images (XMLD-PEEM, LEEM, and morphological PEEM) presented in this paper, on the same sample region. XMLD contrast images are generated from PEEM images collected at two energy point of the Ni L_2 multiplet structures using horizontally polarized (HP) and vertically polarized (VP) light, through standard procedures (by $(I_1-I_2)/(I_1+I_2)$, where I_1 and I_2 are the images obtained at the Ni L_2 edge multiplet energies)[20] and morphological PEEM images are generated just by adding these two energy point images (I_1+I_2). As photons were incident on the sample surface at a grazing angle of 16°, the contrast obtained from XMLD-PEEM with HP light mapping in-plane component of the antiferromagnetic domains while the contrast with VP light largely representing the out-of-plane component. All measurements were performed at room temperature and confirmed by subsequent measurements at different sample regions.

III. RESULTS AND DISCUSSIONS

A. AS-CLEAVED SURFACE

1. Nonequilibrium in-plane and out-of-plane domain structure

We show the images of different experiments on the same area of the as-cleaved surface in Figs. 1(b)–1(f). We can observe different contrast features on the LEEM image of the surface in Fig. 1(b) as indicated by arrows. The PEEM morphological images are shown in Fig. 1(c) with HP light and in Fig. 1(d) with VP light. Observation of similar features (which are polarization independent) in the corresponding regions as in LEEM (indicated by arrows) confirms that morphological PEEM imaging indeed depicts the surface topography. The extra stripes [indicated by arrows in Figs. 1(c) and 1(d)] comes from the surface scratches (possibly from the cleaving process) as evident from different LEEM images [Figs. 1(b) and 2]. XMLD-PEEM image obtained at the Ni L_2 edge in the same location using HP light is displayed in Fig. 1(e) while that obtained using VP light is shown in Fig. 1(f). The black (stripped) regions in VP image [Fig. 1(f)] corresponding to the features in LEEM images, are absent in the image with HP light. Apart from these, we also observe some curved bright regions in HP image [Fig. 1(e)] with larger contrast in comparison to VP image [Fig. 1(f)]. Thus, there is photon polarization dependence in these observed features. Along with the fact that, our surface shows a long-range antiferromagnetic order (from exchange scattered spots in LEED) we can conclude in these XMLD-PEEM images, the origin of the contrast is magnetic in nature and other issues such as charging effects, crystal-field effects[24] have been ruled out. In Fig. 1(e), we see primarily two distinct gray scales (for example, see Fig. 3), each of which is proportional to a $\cos^2\theta$ term, where θ is the angle between the

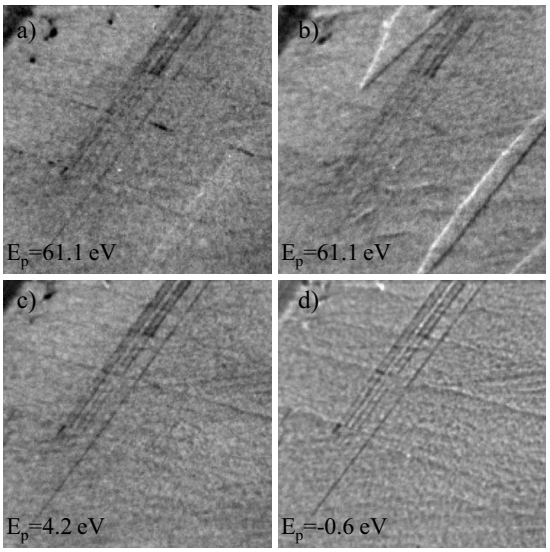

FIG. 2. (a) LEEM image obtained at $Ep=61.1$ eV in the nearly focused and (b) underfocused conditions. (c) LEEM image at 4.2 eV in defocused condition and (d) at −0.6 eV (MEM mode).

photon polarization vector and antiferromagnetic vector (spin-axis direction).[20] In our case, the bright and dark areas on the image present domains where the antiferromagnetic vector makes larger and smaller angle with the polarization vector, respectively. The observed domains in Fig. 1(e) have large in-plane character as probed by HP light. The same in-plane domains can also be observed in Fig. 1(f) using VP light but with a diminished contrast [~20% of Fig. 1(e)] confirming the near in-plane character of the observed surface domain structure. The observed domain pattern on as-cleaved surfaces appears rather curious with curved domain walls. They are very different from what is known on annealed surfaces of NiO single crystals,[20,22] where the surface domains have the bulk symmetry with the domain-wall traces following particular crystallographic directions, representing equilibrium domain structure. There have been some

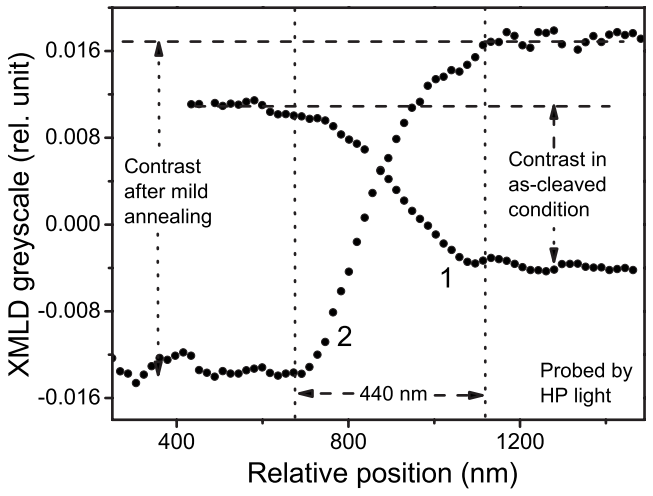

FIG. 3. XMLD gray scale along the line drawn in Figs. 1(e) and 4(a) showing the transition width and in-plane spin reorientations after mild annealing.

earlier observation of curved domain wall on bulk-terminated antiferromagnetic domain structures on NiO single crystals due to the elastic strain field originated by disclinations at the domain-wall boundaries.[15] However, the magnetic domain structure observed on the as-cleaved surfaces appears rather different compared to previous observations.

On bulk-terminated equilibrium domain structure, it is expected to observe domains with $\langle 11\bar{2}\rangle$ spin-axis directions. Effort have been made to associate the observed dichoric gray scales with conventional bulk-terminated domain structure but axes of the antiferromagnetic spins have different behavior compared to the equilibrium bulk-terminated domains and we cannot associate them with the conventional T or S kind of domains. The possible explanation for the behavior of these surface domains could be due to the presence of inhomogeneous surface strain, generated during the cleaving process.[25] This induced surface strain field may influence the magnetic anisotropy of the surface via magnetoelastic effect and can alter the antiferromagnetic spin-axis orientations.[26] The inhomogeneous strain field on the surface may be represented by the fictitious dislocations with infinitesimal Burgers' vector continuously distributed on the surface within the formalism of quasidislocations in magnetoelasticity.[4,27] The induced strain field raises the surface energy density in a laterally inhomogeneous way and the domain walls loose their directionality as they have to satisfy the local compatibility conditions[11,15] to minimize the energy density. Depending on the microelastic properties of the surface, the surface strain and the resulting domain structures could be pinned by defects, dislocations, and grain boundaries.

As mentioned before, apart from the in-plane domain traces, in Fig. 1(f) we also observe extra contrast in the form of dark stripes, which are clearly associated with out-of-plane magnetic domains on the surface as contrast for out-of-plane domains will appear only when VP light is used. This observation of out-of-plane domains is interesting as only in case of tensile strained thin films of NiO(100) grown on MgO(100) is known[8] to possess preferential surface out-of-plane spin configuration. In case of bare NiO crystal surfaces, only conventional domains are known.[20–22] Comparing LEEM image [Fig. 1(b)] or PEEM images [Fig. 1(c) or 1(d)] with Fig. 1(f), we find a one-to-one correspondence between the features observed in LEEM with that of the observed out-of-plane magnetic stripe domains, which is very striking.

2. Origin of the nonequilibrium out-of-plane domain structure

For understanding these out-of-plane domains, the origin of the contrast mechanism in LEEM has to be understood. We show LEEM images taken with $Ep=61.1$ eV in overfocused [see Fig. 1(b)], nearly focused [see Fig. 2(a)] and underfocused [see Fig. 2(b)] conditions and we see the reversing contrast of these stripes with vanishing striped features in the near in-focus condition. This behavior clearly indicates the phase-contrast mechanism at work with surface steps at these striped features. However, in LEEM images below 50 eV, we do not see these striped features in the defocused

condition [see Fig. 2(c) with $Ep=4.2$ eV]. To see the surface topography, we performed mirror electron microscopy (MEM) where the electrons are ballistically reflected by the surface potential just above the surface, as can be seen in Fig. 2(d) with $Ep=-0.6$ eV. In both Figs. 2(c) and 2(d), no striped features can be seen indicating the absence of any atomic steps on the surface and ruling out any morphological origin of the stripes.

In case of thin films grown on substrates, buried interfaces and interfacial dislocations have been observed in LEEM by Tromp *et al.*[28] The interfacial dislocations give rise to extended strain field up to surface of films resulting in displacements of the surface atoms, which can produce interference patterns on the elastically scattered electrons and can be detected by the phase-contrast mechanism in the defocused condition. The contrast in Figs. 1(b) and 2(b) can be understood in a similar manner as in case of thin films; extended strain field originated by the dislocation network buried in the crystal producing surface-atom displacements. However, the contrast represents the surface strain pattern originating from buried dislocations and does not image the dislocations directly. There are few reports[28–30] on the observation of buried interfacial dislocations at the interface between the grown film and substrate but not on bare single crystalline surfaces. In case of line dislocations, the width of the surface displacements is known[30] to be comparable to the depth of the strain nucleus below the surface from which the displacement field occurs. The width of the surface displacement region estimated by the width of the contrast transition (boundary) region of the stripped features [marked by arrows in Fig. 1(b)] is about 150 nm and gives a measure of the depth from the surface where the dislocation network is buried. The displacement field at the surface can be estimated[31] with the phase shift given by $\phi=kd=(2\pi/\lambda)2a_\circ$ where λ is the electron wavelength and $a_\circ$ is the surface step height. From this interference condition at 61 eV with a phase shift of $\pi/2$, we can estimate the surface step height ($a_\circ$) to be around 0.2 Å. As the depth of the buried dislocation from the surface increases, the width of the displacement field increases[32] and the amplitude of the surface-atom displacements decrease owing to the lattice relaxations and damping of dislocation field. The observed step height of 0.2 Å should thus correspond to the magnitude of Burgers vector at the buried dislocation site which to a first order is the interatomic spacing (~2 Å). This also explains why we do not see the dislocation patterns at low energies [Fig. 2(c)], as the phase contrast generated by the step is not detectable at these energies. Thus, the electron primary energy at which the dislocations are visible is a good measure of the depth from the surface at which these dislocations are buried. The ability to detect surface steps[28,30,31] as small as 0.2 Å, which is practically very difficult to observe by any other technique including scanning tunnel microscope over micron length scales, manifests the capability of the LEEM technique. Even though sensitive to surface topography, the MEM [Fig. 2(d)] fails to detect these surface-atom displacements as these steps are below the vertical resolution limit of the instrument (~1–2 Å) as well as the broad features giving rise to weak modulations of the surface potentials. Preferential (average) out-of-plane magnetic spin configurations are stabilized in tensile strained

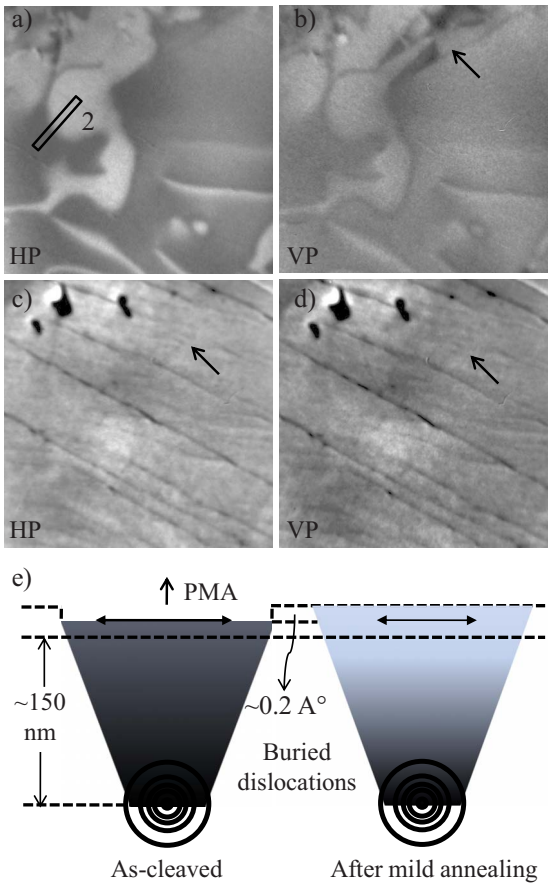

FIG. 4. (Color online) (a) XMLD-PEEM image of the as-cleaved surface using HP light and (b) using VP light after mild annealing. (c) Topography image generated from the PEEM images at the same region with HP light and (d) with VP light after mild annealing. (e) Schematic accounting the effect of strain field caused by buried dislocations (see text for details).

NiO; which is demonstrated both experimentally[8] as well as theoretically.[33] This suggests that the striped domains are regions of lattice where they are expanded in plane while contracted in out-of-plane direction leaving the striped surface 0.2 Å below the rest of the surface. Thus, these black stripes represent strain-induced nonequilibrium out-of-plane AF domains not the conventional bulk-terminated equilibrium domains.

B. EFFECT OF MILD ANNEALING

1. In-plane spin reorientation

If induced strain field (resulting from the cleaving process) is the cause for the nonequilibrium domain structure then the domain structure is expected to be modified by variation in this strain field. By annealing the surface, one provides sufficient thermal energy to overcome different lattice pinning effects and releasing/modifying the nature of surface inhomogeneous strain field. In Figs. 4(a) and 4(b), we show the XMLD-PEEM images of the same area of the surface after it was annealed *in situ* to 473 K (below T_N). The resulting antiferromagnetic domain pattern retains the mor-

phological character as that of the as-cleaved antiferromagnetic domains in Fig. 1(e) with irregular domain shape. However, the domain pattern undergoes changes caused by the changes in the nature of inhomogeneous strain-field pattern resulting from the annealing process. In Fig. 3, we show the line profile along the region 1 [Fig. 1(e)] and region 2 [Fig. 4(a)] to show the changes in XMLD gray scales in more quantitative way. As we can see, the gray level corresponding to dark domain in Fig. 1(e) has moved down and the gray level corresponding to bright domain has moved up after annealing. As mentioned before, for fixed experimental geometry and polarization direction, these changes imply changes in the antiferromagnetic spin-axis direction through an angular dependence. The contrast between these (bright and dark) domains have increased considerably after mild annealing as evident from Fig. 3. After annealing a movement of domain wall has been observed. The domain walls follow the paths to minimize the local magnetoelastic energies, causing a spin reorientation between different in-plane domains as there is no contrast reversal within the images acquired by HP and VP light [compare Fig. 4(a) and 4(b) excepting the region indicated by arrow]. In these observations, the smaller (bright) domains coalesce to form bigger domains, demonstrating the nonequilibrium nature of these domains.

Here, we would like to make some comments about the nonequilibrium domain walls that is the transition region of antiferromagnetic order parameter between two nonequilibrium domains. The domain walls in NiO have been studied in very details by Weber *et al.*,[15] they have explained that the magnetoelastic interaction is the primary factor governing the width, internal structure of domain wall. The realistic value of the domain-wall width (134–184 nm) can be found from the competition between exchange interaction and an effective anisotropy which contains an additional anisotropic magnetoelastic term. In Fig. 3, we show the width of the order-parameter transition region for these kinds of domain walls. One has to remember that nature of these profiles depends on the angular configuration between the polarization vector and the spin configuration inside the domain wall (internal structure of the domain wall). Within some uncertainty (due to pixel to nanometer mapping, finite resolution, line profile averaging procedure and drift correction), the transition width (not the domain-wall width) have been found to be same about 440 nm which is more or less same as reported (see Fig. 3 of Ref. 15) for more equilibrium type domain structure.

2. Out-of-plane to in-plane spin reorientation

The most interesting changes happening in these images are the absence of the black stripped out-of-plane domain regions which were observed in Fig. 1(f). In these regions, the out-of-plane domains have vanished and the spin axis of the antiferromagnetic domains have undergone a spin reorientation from out of plane to in plane. Still some traces of the out-of-plane domains can be seen in Fig. 4(b) (as indicated by arrow) with weaker contrast, suggesting domain switching was not completed in this region. The absence of striped out-of-plane AF domains at the surface suggests that the tensile strained regions have relaxed while regions with weak contrast indicates reduced strain magnitude, possibly the annealing temperature was not sufficient to relax all the surface strain pinned by the surface defects. The morphological PEEM images in Figs. 4(c) and 4(d) also suggest the (near) absence of surface topography.

Now, we will try to understand why this spin reorientation (from out of plane to in plane) occurs. It is possible that the dislocations have either moved further deep or even disappeared by annihilation with other dislocations. However, the annealing temperature used is rather low to enable diffusion of atoms and to mobilize the dislocations, making these situations very unlikely. The situation could be best explained by the schematics shown in Fig. 4(e), which is strongly supported by the large magnetoelastic effects in NiO crystals. Dislocations (the field near dislocation is presented by concentric circles as a singular point or source, which is stronger than the field presented by graded region up to the surface) are buried at distance on the order of 150 nm below the surface of the cleaved crystal and the extended strain-field (depicted by the graded region) propagates to the surface, with decreasing atomic displacement (reduced gray scale), in Fig. 4(e). The surface-atom displacements are rather small ($\sim$0.2 Å) as observed from LEEM, however, is sufficient to give rise to detectable out-of-plane magnetic domain configurations (as a result of PMA coming from the expanded in-plane lattice parameter [represented by the bidirectional arrow on surface in Fig. 4(e), left]. This indicates that the surface strain field is rather weak, given that the dislocations are buried deep below. During the annealing process, the atoms have sufficient thermal energy to relax and to get rid of the strained surface lattice parameter which are not energetically favorable and to return to the surface equilibrium position with reduced in-plane lattice parameter [indicated by the smaller bidirectional arrow in Fig. 4(e), right] with in-plane magnetic domains. After annealing it is unlikely that the relaxation occurs only on the surface to avoid any discontinuous or abrupt changes. It also occurs within the bulk near surface region but not immediate close to dislocation itself. This situation is shown in the "after mild annealing" schematic in Fig. 4(e). These surface structural relaxations are also influenced by other factors such as surface defects, which could result in partial relaxation of the domains as seen by arrow-indicated region in Fig. 4(b). Now the question is what is the origin of these dislocations in the crystal? It is unlikely that dislocations are generated as a result of the cleaving process as then they could be either on or close to the surface. Most likely they were intrinsic to the crystal and it happened that the crystal was cleaved close to them.

IV. SUMMARY

In summary, we have observed nonequilibrium antiferromagnetic domain structure including the presence of PMA (hence out-of-plane domains which are nonconventional by nature) due to the presence of induced inhomogeneous strain field on the cleaved surface of NiO single crystal coming from cleaving process and buried dislocations, respectively. After mild annealing, the antiferromagnetic domain structure

evolves to accommodate the modifications and partial relaxations of the strain field and driving a spin reorientation between different in-plane domains. We also observe a spin reorientation from out-of-plane to in-plane configuration due to changes in perpendicular magnetocrystalline anisotropy after mild annealing. The role of dislocations in modifying many properties of materials such as mechanical and electrical are well known. Here, we show a case where the magnetic properties of an antiferromagnetic surface is strongly modified by the presence of dislocations. The magnetic anisotropy of the surface is modified by the dislocation-induced surface strain field via the strong magnetoelastic effects. Our study shows that magnetoelastic effect is a strong parameter in determining the shape and pattern of the antiferromagnetic domain structure.

ACKNOWLEDGMENTS

S.M. and K.M. gratefully acknowledge the financial support of the International Center for Theoretical Physics (ICTP), Trieste and the Department of Science and Technology, Government of India along with the Italian Ministry of Foreign Affairs for the Synchrotron Radiation studies.

*krishna.menon@saha.ac.in

[1] A. Hubert and R. Schäfer, *Magnetic Domains* (Springer, Berlin, 1998).
[2] S. A. Wolf, D. D. Awschalom, R. A. Buhrman, J. M. Daughton, S. von Molnár, M. L. Roukes, A. Y. Chtchelkanova, and D. M. Treger, Science **294**, 1488 (2001).
[3] I. Žutić, J. Fabian, and S. D. Sarma, Rev. Mod. Phys. **76**, 323 (2004).
[4] H. Gomonay and V. M. Loktev, J. Phys.: Condens. Matter **14**, 3959 (2002).
[5] A. Scholl, M. Liberati, E. Arenholz, H. Ohldag, and J. Stohr, Phys. Rev. Lett. **92**, 247201 (2004).
[6] J. Wu, J. Choi, A. Scholl, A. Doran, E. Arenholz, Y. Z. Wu, C. Won, Chanyong Hwang, and Z. Q. Qiu, Phys. Rev. B **80**, 012409 (2009).
[7] K. De'Bell, A. B. MacIsaac, and J. P. Whitehead, Rev. Mod. Phys. **72**, 225 (2000).
[8] D. Alders, L. H. Tjeng, F. C. Voogt, T. Hibma, G. A. Sawatzky, C. T. Chen, J. Vogel, M. Sacchi, and S. Iacobucci, Phys. Rev. B **57**, 11623 (1998).
[9] Y. Z. Wu, Y. Zhao, E. Arenholz, A. T. Young, B. Sinkovic, C. Won, and Z. Q. Qiu, Phys. Rev. B **78**, 064413 (2008).
[10] T. Yamada, J. Phys. Soc. Jpn. **18**, 520 (1963).
[11] T. Yamada, J. Phys. Soc. Jpn. **21**, 664 (1966).
[12] W. L. Roth, Phys. Rev. **111**, 772 (1958); J. Appl. Phys. **31**, 2000 (1960).
[13] T. Yamada, S. Saito, and Y. Shimomura, J. Phys. Soc. Jpn. **21**, 672 (1966).
[14] K. Nakahigashi, N. Fukuoka, and Y. Shimomura, J. Phys. Soc. Jpn. **38**, 1634 (1975).
[15] N. B. Weber, H. Ohldag, H. Gomonaj, and F. U. Hillebrecht, Phys. Rev. Lett. **91**, 237205 (2003).
[16] D. Alders, J. Vogei, C. Levelut, S. D. Peacor, T. Hibma, M. Sacchi, L. H. Tjeng, C. T. Chen, G. van der Laan, B. T. Thole, and G. A. Sawatzky, Europhys. Lett. **32**, 259 (1995).
[17] F. Nolting, A. Scholl, J. Stöhr, J. W. Seo, J. Fompeyrine, H. Siegwart, J.-P. Locquet, S. Anders, J. Lüning, E. E. Fullerton, M. F. Toney, M. R. Scheinfein, and H. A. Padmore, Nature (London) **405**, 767 (2000).
[18] F. U. Hillebrecht, J. Phys.: Condens. Matter **13**, 11163 (2001).
[19] J. Stöhr, A. Scholl, T. J. Regan, S. Anders, J. Lüning, M. R. Scheinfein, H. A. Padmore, and R. L. White, Phys. Rev. Lett. **83**, 1862 (1999).
[20] F. U. Hillebrecht, H. Ohldag, N. B. Weber, C. Bethke, U. Mick, M. Weiss, and J. Bahrdt, Phys. Rev. Lett. **86**, 3419 (2001).
[21] H. Ohldag, A. Scholl, F. Nolting, S. Anders, F. U. Hillebrecht, and J. Stöhr, Phys. Rev. Lett. **86**, 2878 (2001).
[22] H. Ohldag, G. van der Laan, and E. Arenholz, Phys. Rev. B **79**, 052403 (2009).
[23] P. W. Palmberg, R. E. DeWames, and L. A. Vredevoe, Phys. Rev. Lett. **21**, 682 (1968).
[24] M. W. Haverkort, S. I. Csiszar, Z. Hu, S. Altieri, A. Tanaka, H. H. Hsieh, H.-J. Lin, C. T. Chen, T. Hibma and L. H. Tjeng, Phys. Rev. B **69**, 020408(R) (2004).
[25] F. Guo, H. Sun, T. Okuda, K. Kobayashi, and T. Kinoshita, Surf. Sci. **601**, 4686 (2007).
[26] In-plane domains with $\langle 1\bar{1}0\rangle$ or other possible AF axis directions could be stabilized as a result of the increased surface energy density by the induced strain field.
[27] M. Kléman, J. Appl. Phys. **45**, 1377 (1974).
[28] R. M. Tromp, A. W. Denier van der Gon, F. K. LeGoues, and M. C. Reuter, Phys. Rev. Lett. **71**, 3299 (1993).
[29] P. Sutter and M. G. Lagally, Phys. Rev. Lett. **82**, 1490 (1999).
[30] W. Świech, M. Mundschau, and C. P. Flynn, Appl. Phys. Lett. **74**, 2626 (1999).
[31] W. F. Chung and M. S. Altman, Ultramicroscopy **74**, 237 (1998).
[32] M. Dynna, J. L. Vassent, A. Marty, and B. Gilles, J. Appl. Phys. **80**, 2650 (1996).
[33] M. Finazzi and S. Altieri, Phys. Rev. B **68**, 054420 (2003).